International Journal of Advanced Research and Review

www.ijarr.in

COMPARATIVE FEASIBILITY AND AGING ANALYSIS OF BATTERY TECHNOLOGIES IN HYBRID POWER SYSTEMS CONSIDERING DEMAND VARIABILITY AND CARBON TAX

Musa Terkes[a], Alpaslan Demirci[a*]

Department of Electrical Engineering, Yildiz Technical University, Istanbul, Türkiye
E-mail: [a]musa.terkes@yildiz.edu.tr; [a*]ademirci@yildiz.edu.tr

ABSTRACT

On the road to carbon neutrality, the installation capacity of renewable energy technologies is increasing daily. Due to its inherently intermittent power generation profile, integrating battery energy storage systems (BESS) is critical to ensure a sustainable and reliable energy supply. In a competitive market, high-performance battery technologies developed by many manufacturers will drive the trend toward hybrid power systems (HPS). This paper proposes optimum HPSs with minimum cost for prosumers in the distribution grid using shared BESS, considering battery technologies. Also, the feasibility outputs are compared technically, economically, and environmentally in multi-year sensitivity analyses. Moreover, the impact of daily and hourly simultaneous demand variations is evaluated in aging characteristics for different battery technologies. In addition, the scope of the analysis is deepened by the effects of a high carbon tax on feasibility outcomes in zero carbon tax policies. The results confirm the superiority of NaS battery technology in terms of its financial and renewable potential and LAB benefits for carbon emissions and BESS technical performance. In the later stages, hybrid demand variability further impacts the LAB technology, reducing cycle degradation by up to 7.43% and increasing throughput by up to 11.26%. Additionally, a high carbon tax could reduce CO_2 by up to 9.4% and increase the renewable rate by up to 5.2%. Assessing the feasibility trade-offs in BESS technology selection from multiple perspectives will provide credible win-win environments for stakeholders.

Keywords: Battery technology, battery energy storage, hybrid power systems, demand variability, carbon tax

INTRODUCTION

It has always been essential to minimize cost as much as renewable energy, especially at reasonable reliability levels with load uncertainty. In addition, battery energy storage systems (BESS) that can schedule flexibility services in the long term have become popular. With the advancement of technology, many types of batteries are available today, and their performance varies depending on many conditions. For instance, nickel-cadmium (Ni-Cd) battery technology can achieve a reliability index of 0.32, while ZEBRA and zinc bromide (Zn-Br) can promise the lowest investment and operating costs, respectively (Bakhshi Yamchi et al., 2019). Considering battery degradation in hybrid systems, including photovoltaic panels (PV) and wind turbines (WT), lithium-ion batteries (LIB) instead of lead-acid (LAB), sodium sulfide (NaS), and vanadium redox bromide flux (VRFB) can further increase profitability margins (Yang et al., 2018). Especially in hybrid microgrids, a diesel generator is still the most critical energy alternative at discount rates higher than 1%, while

LIB maintains its superiority in specific ranges of 1-4% (Kebede et al., 2021). However, increasing the discount rate above 4% decreases the interest in LIB and increases the preference for LAB (Ciez & Whitacre, 2016). On the other hand, the minimum incentive tariffs required for different energy storage system (ESS) sizes need to be assessed to attract investors and determine the impact of different battery technologies on the overall cost of energy (Khan et al., 2022). While the additional operating costs related to the degradation characteristics of cycling and calendar aging can compromise affordability, lithium nickel manganese cobalt oxide (NCM) batteries can somewhat reduce this impact (Fallahifar & Kalantar, 2023). Lithium manganese oxide (LMO) battery technology has the advantage of low cost at high throughput. Still, considering the degradation characteristics and power losses based on the state of charge (SOC) and depth of discharge (DOD), the trend toward lithium iron phosphate (LFP) battery technology is increasing (Sayfutdinov et al., 2020). In addition to these obvious features, LFP batteries better address the objectives of reducing electricity costs and the loss of power supply probability (Baumann et al., 2017).

On the other hand, residential batteries can reach profitability before 2030 in applications such as PV self-consumption, load shifting, peak demand reduction, and PV curtailment. Considering geography, lithium nickel cobalt aluminum oxide (NCA) batteries in Austin and NCM batteries in Geneva could offer economical options (Pena-Bello et al., 2019). Moreover, considering the uncertainties in wholesale electricity prices, NaS batteries may promise the most profitable option for sustainable energy capital investment and asset allocation (Mohseni & Brent, 2022). With market price uncertainty, Ni-Cd batteries are unsuitable for microgrids due to their high investment costs and short lifespan. At the same time, LIBs will provide financial savings of up to 18.75% due to their high throughput and long lifespan, despite being more costly than other battery technologies (Mostafa et al., 2020). Considering support services' energy-to-power ratios (duration/SOC range), LIBs and LABs are suggested for short-term services, and NaS and VRFBs for long-term services (Leadbetter & Swan, 2012).

On the contrary, nickel-iron (Ni-Fe) batteries in off-grid rural electrification can support the hybrid system, reducing the lifecycle cost by up to 65% compared to LAB and LIB (P. P. Kumar et al., 2021, 2023). In the islands, Zn-Br batteries promise high returns on investment and renewable penetration, with the advantage of a simple payback period and a green approach (P. Kumar et al., 2021). However, considering a proper energy and battery management strategy, VRFB can maximize the benefits (Merei et al., 2013). Focusing on freshwater availability and electricity demand, Ni-Fe batteries can reduce annual levelized costs (P. P. Kumar & Saini, 2020) and guarantee reasonable performances (Eteiba et al., 2018). However, considering degradation characteristics such as the equivalent cycle model, Rainflow, and Schiffer, LIBs are less costly due to their long lifetime and low maintenance costs (García-Vera et al., 2020). Regarding calendar and cycle aging, VRFBs are the most economical option, but reducing the LIB investment cost below 250 €/kWh may change the preference for ESS (Merei et al., 2014).

On the active distribution network side, besides the uncertainty in energy consumption and generation, the characteristics of the battery parameters may also need to be considered. Zn-Br batteries are the most viable option in such grids, which can reduce environmental and economic concerns, but NaS batteries are an essential alternative considering capacity degradation (Daghi et al., 2016). Integrating energy arbitrage with peak demand reduction and community ESS applications with LIBs or VRFBs can minimize operating costs (Terlouw et al., 2019). In electric vehicle (EV) charging, however, the trend is turning

towards Zn-Br, which can promise the lowest net present cost (NPC) and unit energy prices (Muna & Kuo, 2022). However, LFP batteries are the most suitable option for PV-integrated batteries due to their low-temperature advantages and effective performance in different current profiles (Vega-Garita et al., 2019). On the contrary, choosing Zn-Br batteries in smart hybrid power plants can reduce costs by 66.3% and increase the renewable fraction (RF) by 5% (Sambhi et al., 2023). It proves its superiority over LIBs by reducing environmental concerns by up to 10.1%, especially in cold regions (Li et al., 2020). In large-scale grid applications, the levelized storage cost is 199-941 $/MWh for NaS, 180-1032 $/MWh for LIB, 410-1184 $/MWh for valve-regulated LAB (VRLA), 802-1991 $/MWh for Ni-Cd and 267-3794 $/MWh for VRFB (Rahman et al., 2021). Consequently, considering the spatiotemporal effects of ESSs, VRFBs with high maximum DOD and long discharge duration can guarantee net zero commitment (Huang et al., 2023).

Many literature studies have compared battery technologies under various operating conditions and for different purposes, considering their degradation characteristics. However, the studies have yet to address the shared BESS in distribution networks to which prosumers are connected instead of the use of individual BESS by domestic consumers. Moreover, none of the studies compare the degradation characteristics of different battery technologies and examine the feasibility of a hybrid power system (HPS) in multi-year sensitivity analyses such as increasing electricity tariff, demand, and PV degradation. In addition, battery performances under daily and hourly demand variations have not been analyzed, and the effects of a carbon tax on HPS feasibility have not been addressed. In this context, this study compares VRFB, LAB, NCM, LFP, and NaS batteries in a shared BESS application with multi-year sensitivity analyses. It evaluates the optimum HPS with minimum cost from technical, economic, and environmental perspectives. Arrhenius-based functional, relative capacity versus temperature, cycle-to-failure versus DOD, and life versus temperature curves are considered, and degradation parameters are evaluated simultaneously in aging models. Moreover, aging analyses were performed based on the rainflow counting algorithm and cycle and calendar degradation. Finally, a robust feasibility analysis is validated by considering carbon taxes and daily and hourly demand variability.

MATERIALS AND METHODS

HPS Design and Modeling

Three different mathematical formulations are used in this study, although the PV power generation profile considered in the HPS model is affected by many factors. PV array output power is evaluated in Equation (1), while cell temperatures are determined by Equation (2) to be used in Equation (1). PV efficiency is calculated by Equation (3).

$$P_{PV}(t) = Y_{PV} f_{PV} \left(\frac{G_T(t)}{G_{T,STC}} \right) \left[1 + \alpha_P (T_C(t) - T_{C,STC}) \right] \quad (1)$$

$$T_C(t) = T_a(t) + \left(\frac{G_T(t)}{800} \right) (T_{NOCT} - 20) \quad (2)$$

$$\eta_{mp,STC} = \frac{Y_{PV}}{A_{PV} G_{T,STC}} \quad (3)$$

In particular, data such as solar horizontal irradiation, clearness index, and ambient temperature are taken from the National Aeronautics and Space Administration (NASA) database. Indeed, the average solar horizontal irradiance for Istanbul is 3.94 kWh/m^2/day, the clearness index is 0.481, and the average temperature is 14.46°C.

Based on the degradation background available in the HOMER library, BESSs are evaluated in four technology-independent aging subcategories. In the functional sub-model, the output power is calculated by Equation (4) based on the losses due to possible currents flowing in the circuit, considering the battery's internal resistance. Since the exponential square of the current is included in the equation, the output power decreases with increasing current. By equalizing the derivative of the output power concerning the current flowing through the circuit to zero, the maximum current corresponding to the maximum output power is determined by Equation (5).

$$P_{out} = V_0 I - R_0 I^2 \tag{4}$$

$$I_{Pout,\max} = \frac{V_0}{2R_0} \tag{5}$$

Another sub-model results from the bulk thermal capacity. At each time step, the energy dissipated due to series resistance can be converted into heat or increase the bulk temperature of the tank. The produced heat is transferred to or taken away from the ambient according to the convection equation and is calculated by Equation (6). The internal temperature of the BESS acts according to the energy balance in Equation (7), and the differential solution of the corresponding equation is realized by Equation (8). Based on the relevant equations, HOMER effectively adjusts the SOC_{min} value depending on the available temperature of the battery pack.

$$\dot{Q} = I^2 R \tag{6}$$

$$mc\dot{T} = \dot{Q} - (T - T_a) \tag{7}$$

$$T_{i+1} = (T_i - T_a - \frac{\dot{Q}}{h}) e^{-\frac{h}{mc}dt} + \frac{\dot{Q}}{h} + T_a \tag{8}$$

Another sub-model is used to determine the temperature-dependent relative capacity drop. The sub-model is developed with Equation (9) by fitting the parameters d_0, d_1, and d_2 promised by the battery manufacturers to the study.

$$Capacity(T) = Capacity_{nom}(d_0 + d_1 T + d_2 T^2) \tag{9}$$

Cycle aging, referred to as cycle fatigue in addition to calendar degradation at each time step, regardless of whether the tank is in use or idle, is considered in the last sub-model. Aging is analyzed as a capacity reduction and series resistance increase. The calendar aging is calculated in Equation (10) based on temperature only, while in simple terms, the cycle aging is determined in Equation (11) based on the number of cycles up to the BESS change depending on the DOD. The rainflow counting algorithm converts the SOC-dependent time series into discrete cycles with each DOD, and the cumulative cycle degradation is calculated

from the DOD associated with each cycle in Equation (12).

$$kt = Be^{-\frac{d}{T}} \tag{10}$$

$$1/N = AD^{\beta} \tag{11}$$

$$D = \sum_{i=0}^{N} AD_i^{\beta} \tag{12}$$

In addition to the sub-models, the maximum limits for BESS charging and discharging are also valuable. The maximum power that the BESS can charge during a specific period is determined by Equation (13), while the maximum discharge power is determined by Equation (15), considering the discharge efficiency in Equation (14). Moreover, HOMER imposes two different limitations on the maximum charging power. The first one is related to the maximum charging rate, while the other one considers the maximum charging current and the maximum charging powers are calculated in Equations (16) and (17), respectively. After the three constraints, the maximum charging power is adjusted in the optimization scheme in Equation (18) according to the lowest condition. The maximum storage capacity, capacity ratio, and rate constant limits are also complied with in the battery model, which is considered a two-tank battery model in terms of available and bound energy. Finally, the lifetime energy throughput of the BESS is determined in Equation (19) depending on the maximum capacity and voltage of the storage, the number of cycles until the change, and the DOD.

$$P_{batt,c\max,kbm} = \frac{kQ_1e^{-k\Delta t} + Qkc(1-e^{-k\Delta t})}{1-e^{-k\Delta t} + c(k\Delta t - 1 + e^{-k\Delta t})} \tag{13}$$

$$P_{batt,d\max} = P_{batt,d\max,kbm}\eta_{batt,d} \tag{14}$$

$$P_{batt,d\max,kbm} = \frac{-kcQ_{\max} + kQ_1e^{-k\Delta t} + Qkc(1-e^{-k\Delta t})}{1-e^{-k\Delta t} + c(k\Delta t - 1 + e^{-k\Delta t})} \tag{15}$$

$$P_{batt,c\max,mcr} = \frac{(1-e^{-\alpha_C\Delta t})(Q_{\max} - Q)}{\Delta t} \tag{16}$$

$$P_{batt,c\max,mcc} = \frac{N_{batt}I_{\max}V_{nom}}{1000} \tag{17}$$

$$P_{batt,c\max} = \frac{MIN(P_{batt,c\max,kbm}, P_{batt,c\max,mcr}, P_{batt,c\max,mcc})}{\eta_{batt,c}} \tag{18}$$

$$Q_{lifetime} = f_i d_i (\frac{q_{\max}V_{nom}}{1000W/kW}) \tag{19}$$

Lastly, converters that can operate as inverters and rectifiers are considered to provide energy conversion at AC and DC connection points. Inverter output power is determined in Equation (20), rectifier output power in Equation (21), and converter efficiency in Equation (22).

$$P_{inv}(t) = \eta_{inv} P_{DC}(t) \tag{20}$$

$$P_{rec}(t) = \eta_{rec} P_{AC}(t) \tag{21}$$

$$\eta_{DC/AC} = \frac{P_{PV}}{P_{Converter}} \tag{22}$$

Optimal sizing, technical, economic, and environmental HPS feasibility outputs were performed in the "Hybrid Optimization of Multiple Energy Resources (HOMER Pro)," and the model is shown in

Figure 1. Generally, the optimization inputs are shown in
Figure 1.

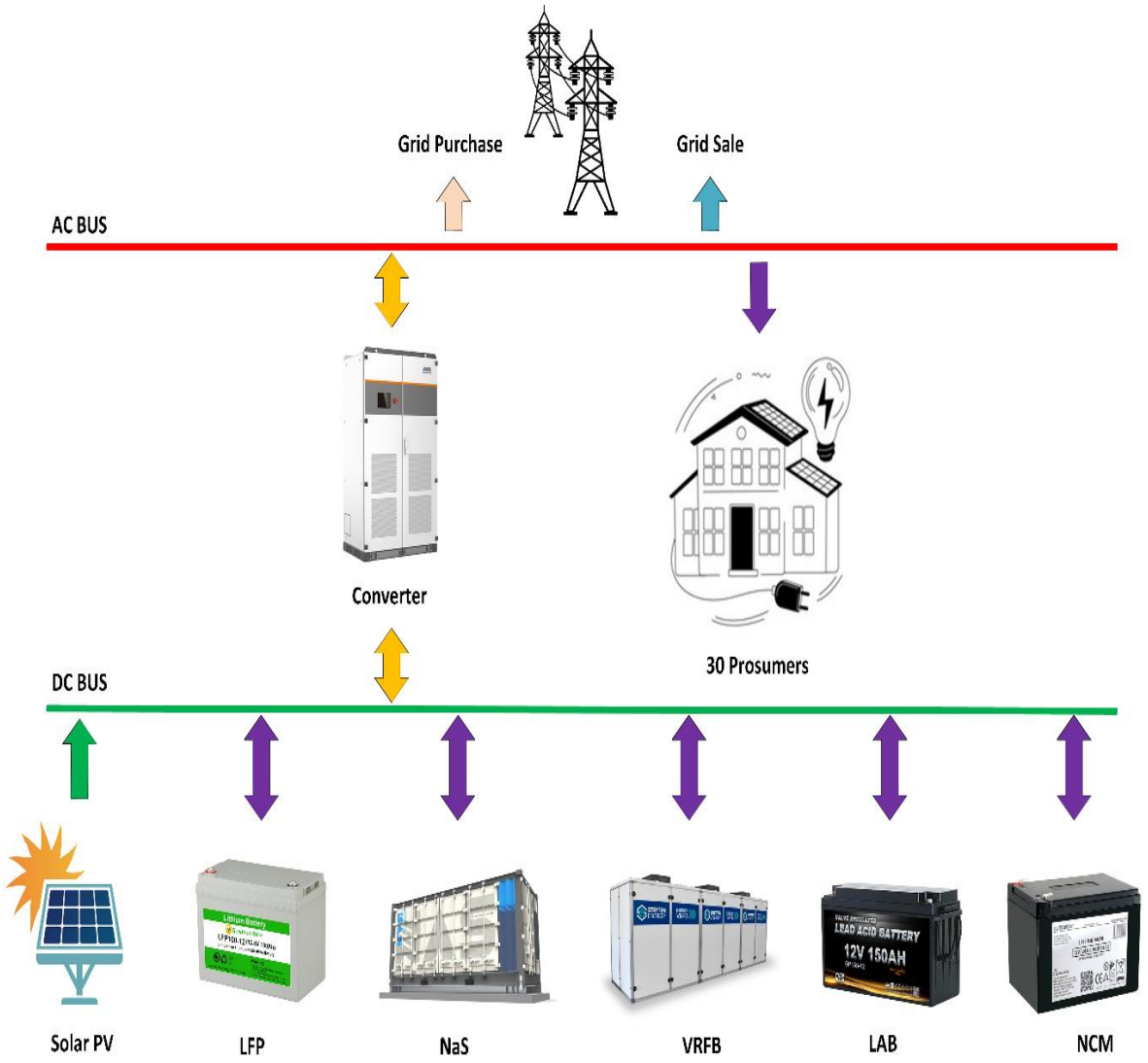

Figure 1. HPS model

Table 1. Optimization inputs of the study

Cost	PV	Converter	LFP	NaS	VRFB	NCM	LAB	
Capital	1500	300	1400	576.6	70	100	115.92	$/kW-h
Replacement	1250	300	1400	576.6	70	100	115.92	$/kW-h
O&M	10	0	7	7.6	0.5	5	9.35	$/kW-h/yr
LOAD								
Peak load	61.76							kW
Demand	300							kWh/day
Load factor	20							%
Variability (day-to-day)	10							%
Variability (timestep)	20							%
GRID								
Flat tariff (06.00-17.00)	0.0822							$/kWh
Peak tariff (17.00-22.00)	0.1199							$/kWh
Valley tariff (22.00-06.00)	0.052							$/kWh
Sell-back	0.01							$/kWh
OTHER								
Inflation rate	14							%
Discount rate	23.3							%
Emission factor in the grid mix	426.1							g/kWh
Project lifetime	20							years
CO_2 tax	20 and 100							$/ton

In this study, WTs are not preferred due to their higher investment costs and installation area limitations, while excess PV power generation is primarily utilized in BESSs. Residual energy that cannot be used in BESSs is sold to the grid, while electricity is purchased from the grid when there is no PV power generation and the BESS is fully discharged. The electricity demand considered in the study originates from 30 prosumers using a shared BESS connected to a common distribution line bus. Regarding battery technologies, LFP, NaS, and NCM batteries, VRFBs, and LABs are considered. The Load Following scheme is chosen as the optimization controller serving the primary load with the lowest total cost at each time step while complying with the operating reserve constraints of the system's controllable power sources (generators, grid, and storage bank). The analyses are performed on a multi-year basis considering cumulative incremental PV degradation (0.5%), grid tariff (3.5%), and electricity demand (2.5%). Finally, the technical inputs of the battery technologies considered in the study are given in Table 2.

Scenarios of the Study

This study compares the feasibility results of LFP, VRFB, NCM, NaS, and LAB technologies in the shared BESS for technical, economic, and environmental aspects in multi-year sensitivity analyses in depth. Moreover, the impact of daily and hourly simultaneous worst-case hybrid demand variability on BESS aging characteristics is evaluated for the selected technologies. In addition, the possible technical, economic, and environmental outcomes of a high carbon tax on HPSs and its impact on the aging characteristics of BESS technologies are investigated concerning the base case. Overall, all analyses utilize optimal HPS capacities sized at minimum cost. The scenarios carried out in the study are shown in Table 3.

Table 2. Comparison of BESS technologies

Parameters	**LFP**	**NaS**	**VRFB**	**NCM**	**LAB**	
Manufacturer	Sunlight	NGK Insulator	UET Reflex	EST Floattech	Hitachi	
$SOC_{initial}$	100	100	100	100	100	%
SOC_{min}	20	20	20	20	20	%
Replacement degradation limit	-	-	50	50	50	%
Maximum C-rate	-	-	-	1 C	0.6 C	A/Ah
Other round-trip losses	-	-	20	4	15	%
Maximum charge current	75	300	80	250	16.67	A
Maximum discharge current	75	800	80	300	24.33	A
Maximum capacity	-	-	164.26	20.19	41.67	Ah
Rate constant	-	-	0	65.26	0.36	1/hr
Capacity ratio	-	-	0.63263	1	0.40	
Effective series resistance	-	-	0.40467	0	0.2819	Ω
Nominal voltage	51.2	12	48	52	24	V
Nominal capacity	5.12	2.2	1.05	7.88	1	kWh
Round-trip efficiency	98	85	-	-	-	%
Lifetime throughput	19200	16061	-	-	-	kWh
Float life	10	20	-	-	-	years
Maximum operating temperature	-	-	45	45	40	°C
Minimum	-	-	0	0	0	°C

Parameters	LFP	NaS	VRFB	NCM	LAB	
operating temperature						
Mass	-	-	38.07	9.08	9.08	kg
Fixed bulk temperature	-	-	38	23	25	°C
d_0	-	-	0.923	0.82985	0.79515	
d_1	-	-	0.00345	0.0089608	0.011961	
d_2	-	-	-0.0000375	-0.000094384	-0.00011212	
A	-	-	0.00017773	0.00010479	0.00013264	
β	-	-	2.03	1.44	1.02	
B	-	-	3.17	3.17	5391.07	
d	-	-	3826.71	3826.71	6368.28	

Table 3. Scenarios of the study

Scenarios	BESS technologies					Demand variability (±%)		CO_2 tax ($/ton)	Feasbility	Aging analysis
	LFP	NaS	VRFB	LAB	NCM	Day-to-day	Timestep			
A	✓	✓	✓	✓	✓			20	✓	
B				✓	✓	30		20		✓
C		✓		✓	✓			20 & 100	✓	✓

Objective Functions and Decision Criteria

The main objective of this study is the evaluation of different battery technologies in BESS and the comparative analysis of HPS feasibility outputs. Firstly, the HPS needs to be optimally sized to address the related objective. Accordingly, minimization of NPC is set as the first objective, while at the same time, lower COE is desired. In addition, increasing the renewable potential and reducing carbon emissions are other goals in the transition to sustainable carbon-neutral cities.

The NPC can be calculated by subtracting revenues from financial cash flows at the end of each year, summing the difference, and discounting it to the present. The capital recovery factor is determined as in Equation (23) to perform the calculation procedure depending on the real discount rate and the project life. Then, the NPC can be calculated as in Equation (24). With the determined NPC, the COE ratio of the annual electricity generation cost to the electricity load served can be calculated in Equation (25).

$$CRF(i,N) = \frac{i(1+i)^n}{i(1+i)-1} \tag{23}$$

$$NPC = \frac{\frac{TAC_{HPS}}{CRF}}{\frac{i(1+i)^n}{(1+i)^n-1}} \tag{24}$$

$$COE = \frac{CRF(i, R_{proj})NPC}{E_{served}} \tag{25}$$

The share of renewable energy generation in electricity demand is calculated in Equation (26), while the cumulative carbon emissions are determined in Equation (27), considering the emission factor in the grid mix.

$$RF = (1 - \frac{E_{non-ren.}}{E_{load}})100 \tag{26}$$

$$TCO_2 = \sum_{t=1}^{n} (CO_2)_t (EF_{grid})_t \tag{27}$$

The share of PV energy transferred directly to load in total PV energy generation is known as the self-consumption ratio (SCR) and is calculated using Equation (28). In contrast, the share of PV energy transferred directly to the load in the total electricity demand is known as the self-supply ratio (SSR) and is calculated using Equation (29). For proper sizing of the HPS, a higher excess of electricity is not desirable. Accordingly, the share of excess electricity in the total electricity generation, i.e., the curtailed energy (CE), is calculated by Equation (30).

$$SCR = \frac{\sum E_{PV}^{cons}}{\sum E_{PV}^{gen}} \tag{28}$$

$$SSR = \frac{\sum E_{PV}^{cons}}{\sum E_{load}} \tag{29}$$

$$CE = \frac{E_{excess}}{E_{production}} \tag{30}$$

The storage wear cost, characterizing the energy cycle cost, is calculated annually in Equation (31). In contrast, autonomy, the ratio of storage bank size to electrical load, is determined in Equation (32).

$$C_{bw} = \frac{C_{rep,batt}}{N_{batt} Q_{lifetime} \sqrt{\eta_{rt}}} \tag{31}$$

$$Autonomy = \frac{N_{batt} V_{nom} Q_{nom} (1 - \frac{q_{\min}}{100})(24h/d)}{L_{prim,ave}(1000Wh/kWh)} \tag{32}$$

OPTIMIZATION RESULTS

The effect of BESS technologies on the feasibility of HPS is evaluated in Figure 2. Considering the optimal capacities with minimum cost, the PV capacity is as high as 35.54%, and the converter capacity is as high as 38.33% for NaS battery technologies. In contrast, the BESS capacity has the highest installation in LAB technology. Although the capital expenditure (CAPEX) increases by up to 35.54% due to higher PV and converter capacity, the HPS costs (NPC and COE) proposed for NaS battery technologies are up to 28.4% lower. The higher revenue from the sale of electricity to the grid compensates the CAPEX to a certain extent, while the increase of RF up to 18.5% maximizes the benefit. Indeed, lower SCR and higher SSR up to 29.14%, although not as high as VRFB, increase the trend towards NaS battery technology. However, the residual energy caused by high RF and SSR and low

SCR is lower in LABs by up to 4.15%. They also release up to 46.89% less carbon than NaS battery technologies despite their renewable potential advantages with lifetime throughput of up to 94.6%, autonomy of up to 11.84 hours, and low storage wear cost of up to 55.66%. However, LFP and VRFB technologies have the lowest BESS losses.

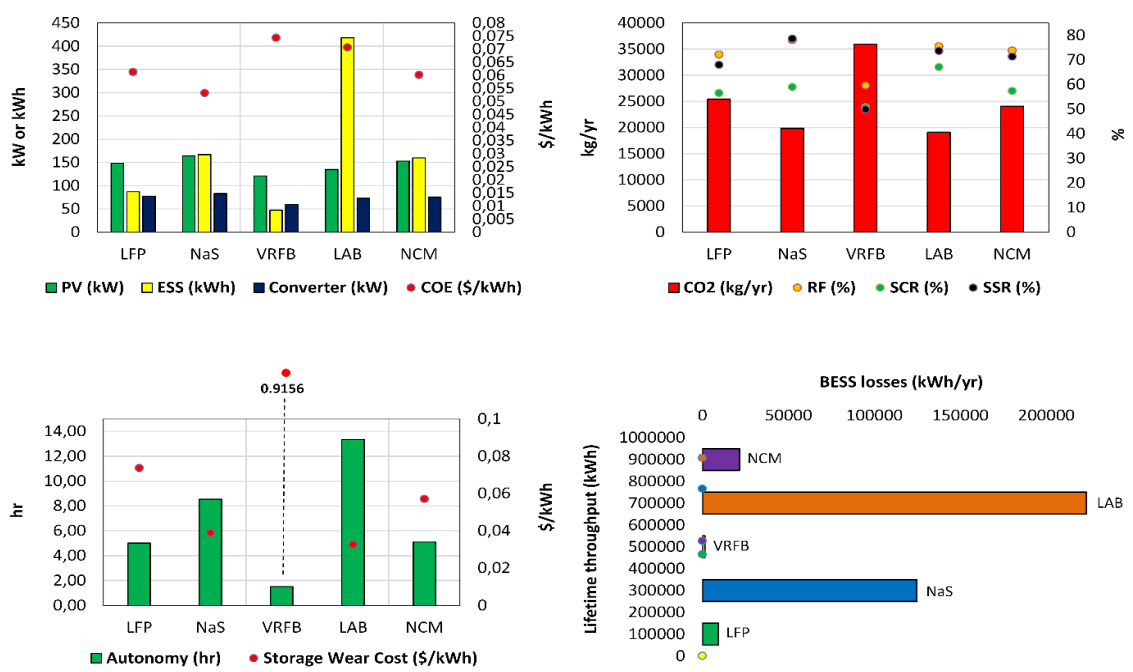

Figure 2. Impact of BESS technologies on HPS feasibility

As the aging analysis can be better elaborated in the optimization framework, the effects of daily and hourly simultaneous demand variability (±30%) on HPS feasibility are shown in Figure 3 for LAB and NCM technologies.

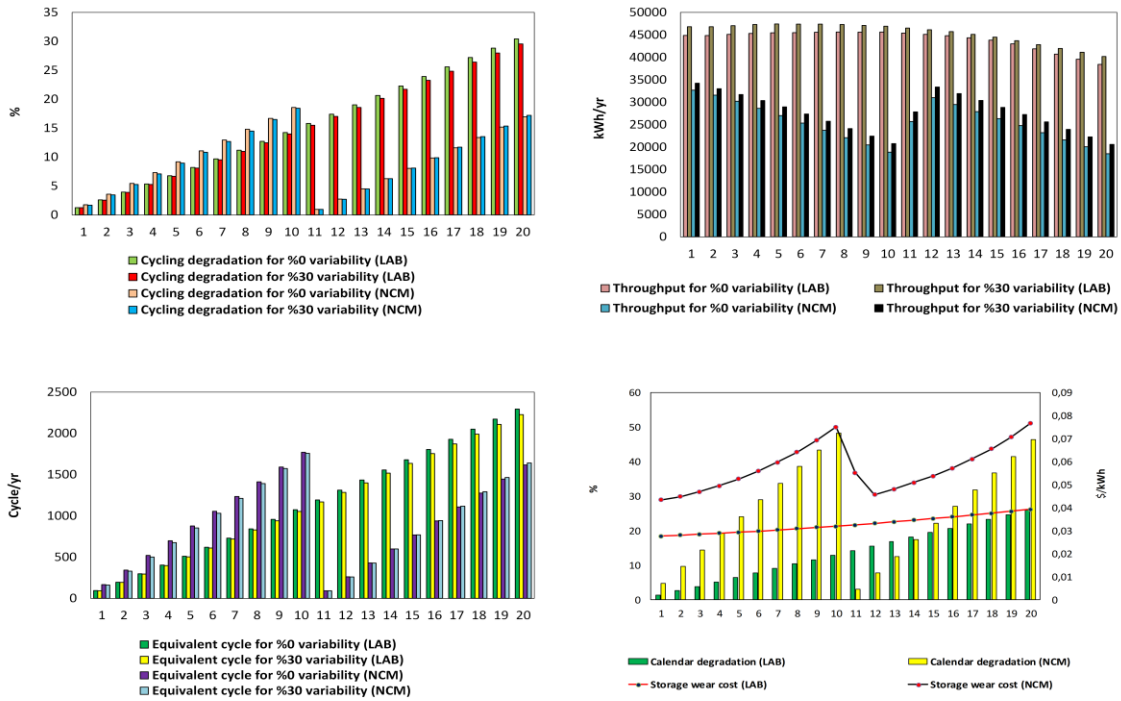

Figure 3. The impact of daily and hourly simultaneous demand variability on aging considering BESS technologies

After hybrid demand variability, further temperature-related calendar degradation does not effectively increase or decrease. Considering LAB technologies, hybrid demand variability reduces cycle degradation by up to 0.88% per year and up to 7.43% in total. It also reduces the number of cycles by 66.49 and 561 per year and the total number of cycles, respectively. The main reason underlying fewer cycles is due to higher throughput. More specifically, the annual and total throughput increases up to 4.58% (1969 kWh/year) and 3.26% (28,69 kWh). Accordingly, the autonomy increases up to 14.44 hours while BESS losses of up to 5.12% cannot be eliminated. It should be noted that the storage wear cost remains unchanged, especially for LAB technology.

On the other hand, considering NCM technologies, hybrid demand variability reduces annual and total cycle degradation by up to 0.32% and 1.22%. It also reduces the number of cycles by 24.61 and the total number of cycles by 109.27. More significantly, the throughput increases up to 11.26% (2496 kWh/year) and up to 8.15% in total (41,49 kWh). Accordingly, autonomy increases up to 6.71 hours, while BESS losses of up to 11.26% cannot be eliminated. In contrast to LAB, it can be noted that the storage wear cost decreases up to 4.05%. Finally, for NCM technology, cycle degradation, and cycle counts are less affected by hybrid demand variability, while parameters such as throughput and storage wear cost are more affected.

Finally, the aging performance of LAB and NCM technologies should also be compared. In terms of calendar degradation, the NCM battery technology degrades up to 35.22% more over the years, while lifetime BESS replacement occurs once between years 10 and 11. The cycle degradation of up to 4.45% per year and the equivalent cycle of up to 704.46 cycles is higher for the NCM until the replacement occurs, while after the replacement, the disadvantage shifts to the LAB. LABs outperform NCM by 27.18% in total equivalent cycles, 73% in total throughput, 10.61% in autonomy, and up to 57.47% in storage wear cost. In return, however, BESS losses are up to 90.39% lower for NCM. Increased demand variability makes the differences more significant.

Figure 4 shows the beneficial impact of a high carbon tax on HPS feasibility for BESS technologies. Higher carbon taxes affect LAB technology the most in terms of capacity installations. Therefore, PV capacity increases by up to 29.63%, BESS capacity by up to 12.44%, and converter capacity by up to 15.62%. Due to the beneficial effects of higher capacity installations, CAPEX increases up to 29.63% while NPC decreases up to 7.37% and COE decreases up to 18.61%. For NPC, NaS is the BESS technology for which the carbon tax is most effective, while for COE and CAPEX, the effect favors LAB. In contrast, considering the renewable potential, a higher carbon tax increases the RF by up to 5.2% and the SSR by up to 7.17% while reducing the SCR by up to 10.3%. Accordingly, CO_2 can be reduced by up to 9.39% in NaS technology, although the carbon tax affects LAB technology more. Regarding autonomy, storage wear cost, and lifetime throughput, the effects of the carbon tax vary (± %). However, for NCM technology, it can be said that BESS losses and the associated lifetime throughput increase up to 12.1%. Moreover, higher carbon taxes can increase the total equivalent cycle by 371.06 for LAB and 50.48 for NCM technology.

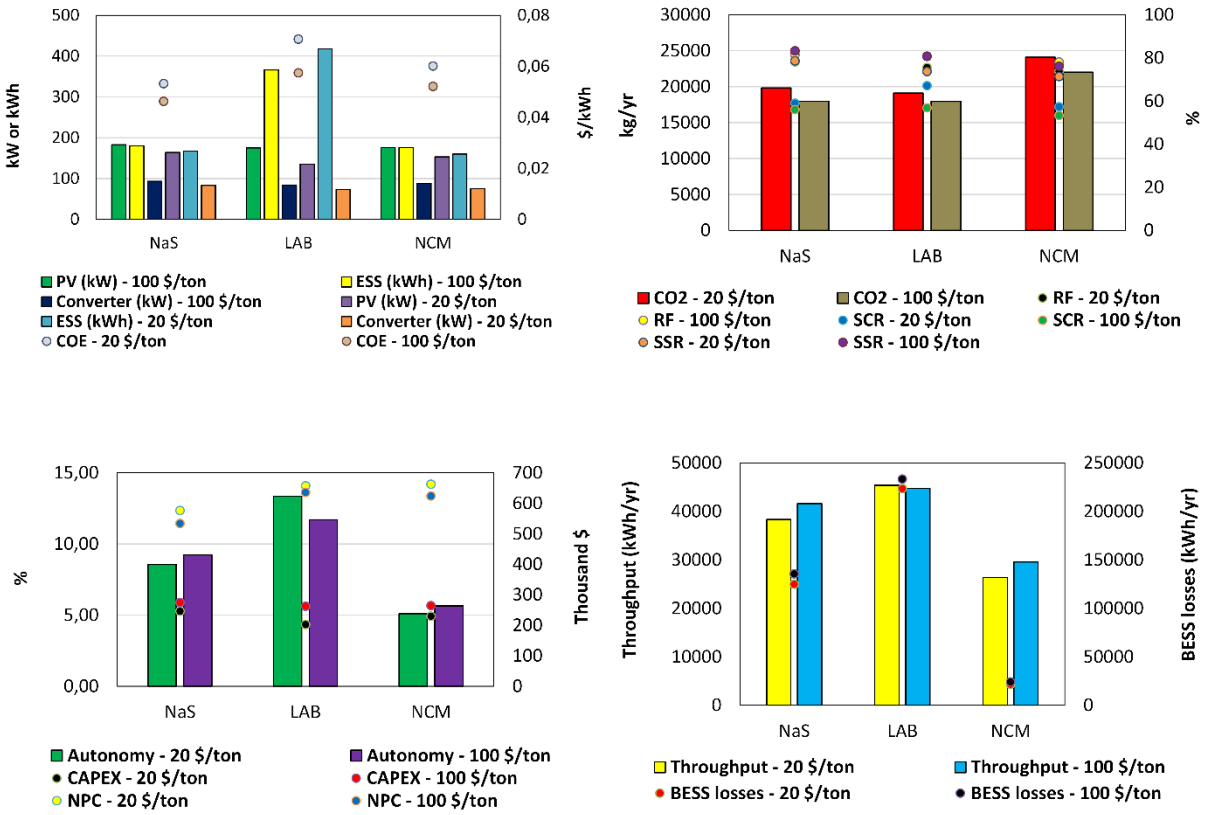

Figure 4. Impact of a higher carbon tax on HPS feasibility considering BESS technologies

CONCLUSIONS

In this study, minimum-cost HPSs are optimally sized for a distribution grid of prosumers using a shared BESS, and their technical, economic, and environmental feasibility results are evaluated in multi-year sensitivity analyses. HPS outcomes for NaS, VRFB, LFP, NCM, and LAB technologies are comparatively analyzed. At the same time, the impact of daily and hourly simultaneous hybrid demand variability and high carbon tax on BESS aging performance and feasibility are also considered. Multi-year sensitivity analyses consider increasing electricity demand, grid tariff, and PV degradation and improve the reliability of feasibility analyses with four different sub-aging schemes using Arrhenius and Rainflow Counting strategies. The results confirm the superiority of NaS battery technology for capacity installations, NPC, COE, CAPEX, RF, SCR, and SSR parameters, and LAB technology for CE, CO_2, autonomy, storage wear cost, throughput, and BESS losses. In the following stage, the hybrid demand variability is evaluated. The relevant increases in the parameter reduce the cycle degradation by up to 7.43% and the equivalent cycle by up to 561 while raising the throughput by up to 11.26% and affecting LAB technologies more. In the final stage, higher carbon taxes reduce COE by up to 18.61% and CO_2 by up to 9.4% while increasing RF by up to 5.2% and throughput by up to 12.1%. Considering that BESS technologies significantly impact the prosumer cost-benefit relationship, the findings of this study could be helpful for many stakeholders. Moreover, depending on the parameters related to aging characteristics, the scope can be extended to hybrid energy storage technologies with various policies to be included in the study on the path to carbon neutrality.

ACKNOWLEDGMENT
Analyzes and comments made in this document belong to the authors. Any institution, company, etc., does not support the article.

DECLARATION OF ETHICAL STANDARDS
The authors of the submitted paper declare that nothing necessary for achieving the paper requires ethical committee and/or legal-special permissions.

CONTRIBUTION OF THE AUTHORS
Musa Terkes: Conceptualization, Software, Data curation, Visualization, Writing-original draft.
Alpaslan Demirci: Supervision, Validation, Investigation, Writing - review & editing.

CONFLICT OF INTEREST
There is no conflict of interest in this study.

REFERENCES
Yamchi, H.B., Shahsavari, H., Kalantari, N.T., Safari, A., Farrokhifar, M., 2019. A cost-efficient application of different battery energy storage technologies in microgrids considering load uncertainty. Journal of Energy Storage. 22, 17-26.
Baumann, M., Peters, J., Weil, M., Marcelino, C., Almeida, P., Wanner, E., 2017. Environmental impacts of different battery technologies in renewable hybrid micro-grids. IEEE PES Innovative Smart Grid Technologies Conference (ISGT) Europe. 1-6.
Ciez, R.E., Whitacre, J.F., 2016. Comparative techno-economic analysis of hybrid micro-grid systems utilizing different battery types. Energy Conversion and Management. 112, 435-444.
Daghi, M., Sedghi, M., Ahmadian, A., Aliakbar-Golkar, M., 2016. Factor analysis based optimal storage planning in active distribution network considering different battery technologies. Applied Energy. 183, 456-469.
Eteiba, M.B., Shimaa, B., Samy, M.M., Wahba, W.I., 2018. Optimization of an off-grid PV/Biomass hybrid system with different battery technologies. Sustainable Cities and Society. 40, 713-727.
Fallahifar, R., Kalantar, M., 2023. Optimal planning of lithium ion battery energy storage for microgrid applications: Considering capacity degradation. Journal of Energy Storage. 57, 106103-106113.
Garcia-Vera, Y.E., Dufo-López, R., Bernal-Agustín, J.L., 2020. Optimization of isolated hybrid microgrids with renewable energy based on different battery models and technologies. Energies. 13, 581-597.
Huang, W.C., Zhang, Q., You, F., 2023. Impacts of battery energy storage technologies and renewable integration on the energy transition in the New York State. Advances in Applied Energy. 9, 100126-100145.
Kebede, A.A., Coosemans, T., Messagie, M., Jemal, T., Behabtu, H.A., Mierlo, J.V., Berecibar, M., 2021. Techno-economic analysis of lithium-ion and lead-acid batteries in stationary energy storage application. Journal of Energy Storage. 40, 102748-102766.
Khan, A.A.M., Farooq, Z., Durrani, A. M., 2022. Techno-economic evaluation of on-grid battery energy storage system at Peshawar using Homer Pro. International Conference on Emerging Technologies in Electronics, Computing and Communication (ICETECC). 1–6.
Kumar, P.P., Rahman, A., Nuvvula, R.S.S., Colak, I., Muyeen, S.M., Shezan, S.A., Shafiullah, G.M., Ishraque, M.F., Hossain, M.A., Alsaif, F., Elavarasan, R.M., 2023. Using energy conservation-based demand-side management to optimize an off-grid integrated renewable energy system using different battery technologies. Sustainability. 15, 10137-

101159.
Kumar, P.P., Saini, R.P., 2020. Optimization of an off-grid integrated hybrid renewable energy system with different battery technologies for rural electrification in India. Journal of Energy Storage. 32, 101912-101934.
Kumar, P.P., Suresh, V., Jasinski, M., Leonowicz, Z., 2021. Off- grid rural electrification in India using renewable energy resources and different battery technologies with a dynamic differential annealed optimization. Energies. 14, 5866-5886.
Kumar, P., Pal, N., Sharma, H., 2021. Techno-economic analysis of solar photo-voltaic/diesel generator hybrid system using different energy storage technologies for isolated islands of India. Journal of Energy Storage. 41, 102965-102986.
Leadbetter, J., Swan, L.G., 2012. Selection of battery technology to support grid-integrated renewable electricity. Journal of Power Sources. 216, 376–386.
Li, C., Zhou, D., Wang, H., Lu, Y., Li, D., 2020. Techno-economic performance study of stand-alone wind/diesel/battery hybrid system with different battery technologies in the cold region of China. Energy. 192, 116702-116714.
Merei, G., Berger, C., Sauer, D.U., 2013. Optimization of an off-grid hybrid PV-Wind-Diesel system with different battery technologies using genetic algorithm. Solar Energy. 97, 460–473.
Merei, G., Magnor, D., Leuthold, M., Sauer, D.U., 2014. Optimization of an off-grid hybrid power supply system based on battery aging models for different battery technologies. International Telecommunications Energy Conference (INTELEC). 1–6.
Mohseni, S., Brent, A.C., 2022. Quantifying the effects of forecast uncertainty on the role of different battery technologies in grid-connected solar photovoltaic/wind/micro-hydro micro-grids: An optimal planning study. Journal of Energy Storage. 51, 104412-104430.
Mostafa, M.H., Aleem, S.H.E.A., Ali, S.G., Abdelaziz, A.Y., Ribeiro, P.F., Ali, Z.M., 2020. Robust energy management and economic analysis of microgrids considering different battery characteristics. IEEE Access. 8, 54751–54775.
Muna, Y.B., Kuo, C.C., 2022. Feasibility and techno-economic analysis of electric vehicle charging of PV/Wind/Diesel/Battery hybrid energy system with different battery technology. Energies. 15, 4364-4383.
Pena-Bello, A., Barbour, E., Gonzalez, M.C., Patel, M.K., Parra, D., 2019. Optimized PV-coupled battery systems for combining applications: Impact of battery technology and geography. Renewable and Sustainable Energy Reviews. 112, 978–990.
Rahman, M.M., Oni, A.O., Gemechu, E., Kumar, A., 2021. The development of techno-economic models for the assessment of utility-scale electro-chemical battery storage systems. Applied Energy. 283, 116343-116357.
Sambhi, S., Sharma, H., Bhadoria, V., Kumar, P., Chaurasia, R., Fotis, G., Vita, V., 2023. Technical and economic analysis of solar PV/Diesel generator smart hybrid power plant using different battery storage technologies for SRM IST, Delhi-NCR Campus. Sustainability (Switzerland). 15, 3666-3688.
Sayfutdinov, T., Patsios, C., Vorobev, P., Gryazina, E., Greenwood, D.M., Bialek, J.W., Taylor, P.C., 2020. Degradation and operation-aware framework for the optimal siting, sizing, and technology selection of battery storage. IEEE Transactions on Sustainable Energy. 11, 2130–2140.
Terlouw, T., AlSkaif, T., Bauer, C., Sark, W.V., 2019. Multi-objective optimization of energy arbitrage in community energy storage systems using different battery technologies. Applied Energy. 239, 356–372.
Vega-Garita, V., Hanif, A., Narayan, N., Ramirez-Elizondo, L., Bauer, P., 2019. Selecting a suitable battery technology for the photovoltaic battery integrated module. Journal of Power Sources. 438, 227011-227021.

Yang, Y., Menictas, C., Bremner, S., Kay, M., 2018. A comparison study of dispatching various battery technologies in a hybrid PV and wind power plant. IEEE Power and Energy Society General Meeting (PESGM). 1–5.